
On the Multiscale Design of Task-Oriented Reflectarrays

G. Oliveri, A. Gelmini, A. Polo, N. Anselmi, and A. Massa

ELEDIA Research Center

Contents

1 Phoenix Patch Reflectarray: 30x30 SLL=-25dB	4
1.1 Optimization target	4
1.2 Optimization results	4
1.2.1 Cost Function	4
1.2.2 Geometrical Design	5
1.2.3 Reflection Coefficient	6
1.2.4 Superficial Currents	7
1.2.5 Fields	7
1.2.6 Fields Cut	8
2 Phoenix Patch Reflectarray: 35x35 SLL=-25dB	9
2.1 Optimization target	9
2.2 Optimization results	9
2.2.1 Cost Function	9
2.2.2 Geometrical Design	10
2.2.3 Reflection Coefficient	11
2.2.4 Superficial Currents	12
2.2.5 Fields	12
2.2.6 Fields Cut	13
3 Double Layer Square Patch Reflectarray: 29x29	14
3.1 Unit cell geometry	14
3.2 Optimization target	14
3.3 Optimization results	15
3.3.1 Cost Function	15
3.3.2 Geometrical Design	15
3.3.3 Reflection Coefficient	16
3.3.4 Superficial Currents	17
3.3.5 Fields	17
3.3.6 Fields Cut	18
4 Double Layer Square Patch Reflectarray: 29x29, Similarity Weight=10	19
4.1 Optimization target	19

4.2	Optimization results	19
4.2.1	Cost Function	19
4.2.2	Geometrical Design	20
4.2.3	Reflection Coefficient	21
4.2.4	Superficial Currents	22
4.2.5	Fields	22
4.2.6	Fields Cut	23

ELEDIA Research Center

1 Phoenix Patch Reflectarray: 30x30 SLL=-25dB

1.1 Optimization target

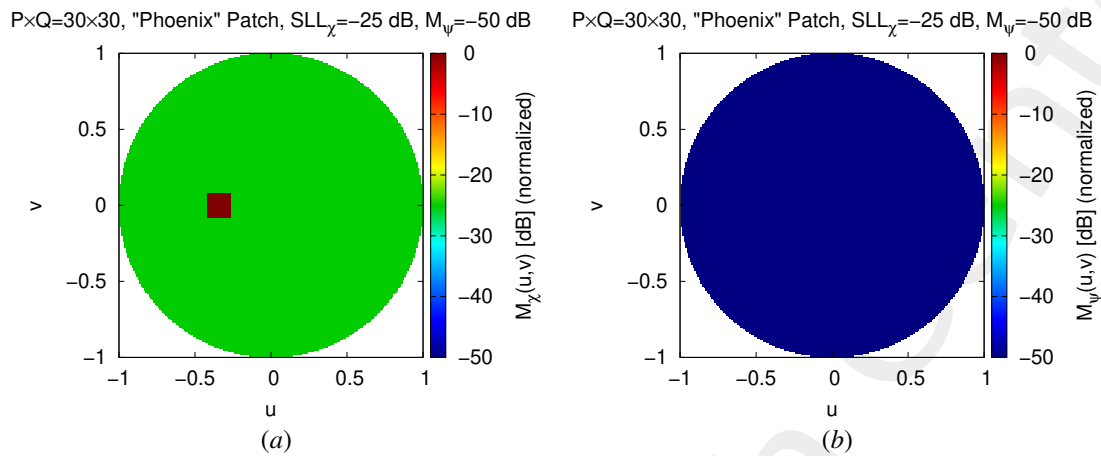


Figure 1: Phoenix Patch Reflectarray 30 × 30 SLL=-25 dB - Optimization target: SLL on the wanted polarization(a), mask on the unwanted polarization (b).

1.2 Optimization results

1.2.1 Cost Function

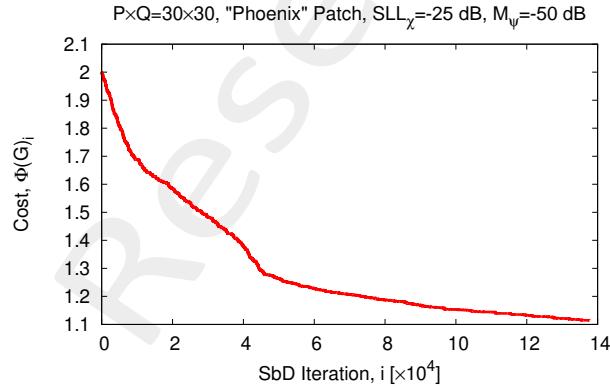


Figure 2: Phoenix Patch Reflectarray 30 × 30 SLL=-25 dB - Optimization: Cost function behavior.

1.2.2 Geometrical Design

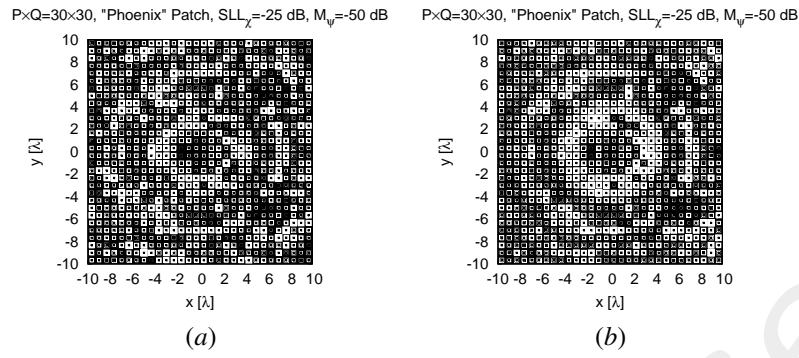


Figure 3: Phoenix Patch Reflectarray 30×30 SLL=-25 dB - Optimization: Starting reflectarray configuration(a) and optimized reflectarray configuration (b).

1.2.3 Reflection Coefficient

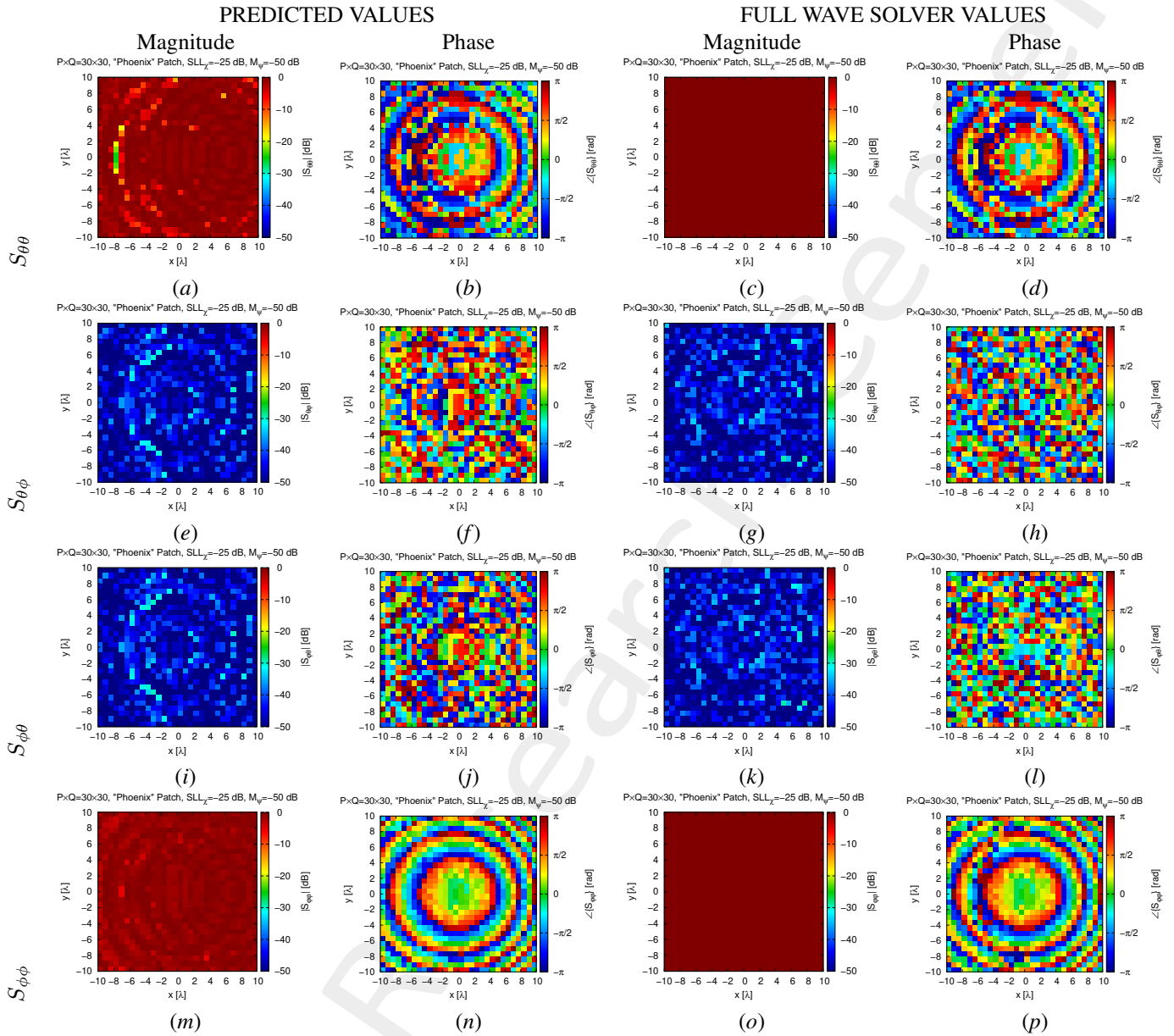


Figure 4: Phoenix Patch Reflectarray 30×30 SLL=-25 dB - Optimization - Reflection Coefficients: predicted(a)(b)(e)(f)(i)(j)(m)(n) vs. full-wave simulation (c)(d)(g)(h)(k)(l)(o)(p) of the magnitude(a)(c)(e)(g)(i)(k)(m)(o) and phase (b)(d)(f)(h)(j)(l)(n)(p) of $S_{\theta\theta}$ (a)(b)(c)(d), $S_{\theta\phi}$ (e)(f)(g)(h), $S_{\phi\theta}$ (i)(j)(k)(l) and $S_{\phi\phi}$ (m)(n)(o)(p).

1.2.4 Superficial Currents

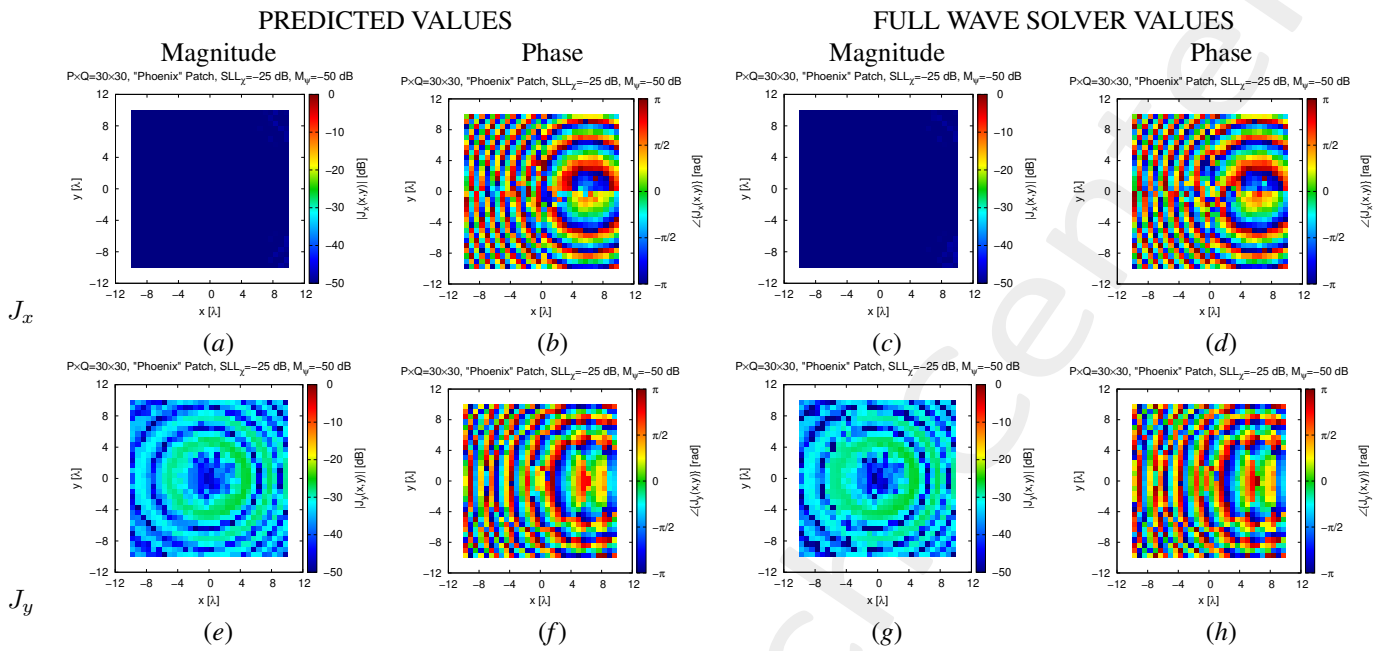


Figure 5: Phoenix Patch Reflectarray 30×30 SLL=-25 dB - Optimization - Superficial Currents: predicted(a)(b)(e)(f) vs. full-wave simulation (c)(d)(g)(h) of the magnitude(a)(c)(e)(g) and phase (b)(d)(f)(h) of J_x (a)(b)(c)(d) and J_y (e)(f)(g)(h).

1.2.5 Fields

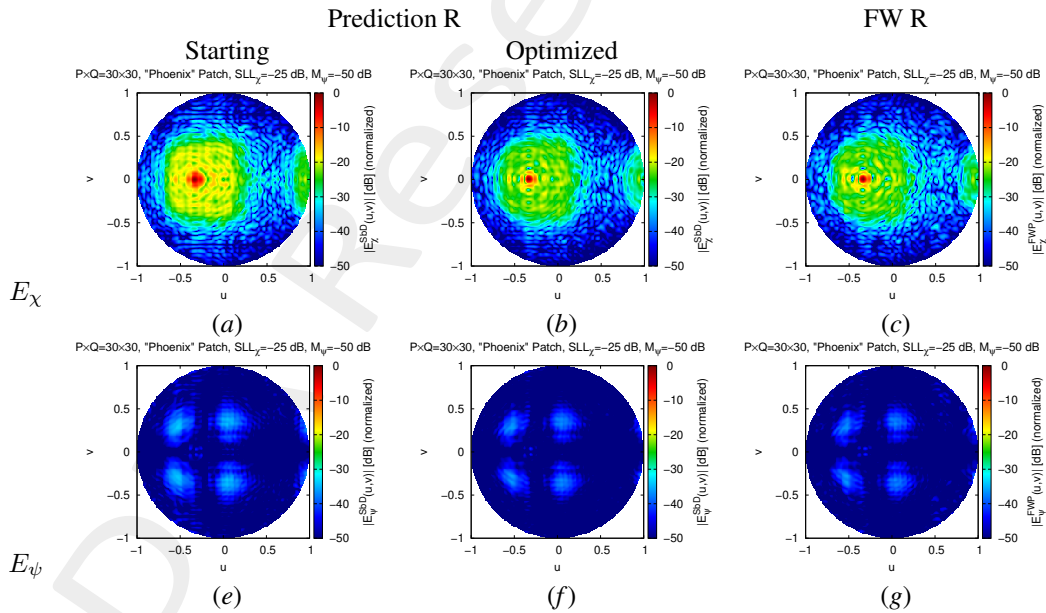


Figure 6: Phoenix Patch Reflectarray 30×30 SLL=-25 dB - Optimization - Radiated Fields: predicted(a)(b)(e)(f) vs. full-wave simulation of R (c)(g) vs. full-wave simulation of the entire structure (d)(h) of the magnitude of E_χ (a)(b)(c)(d) and E_ψ (e)(f)(g)(h).

1.2.6 Fields Cut

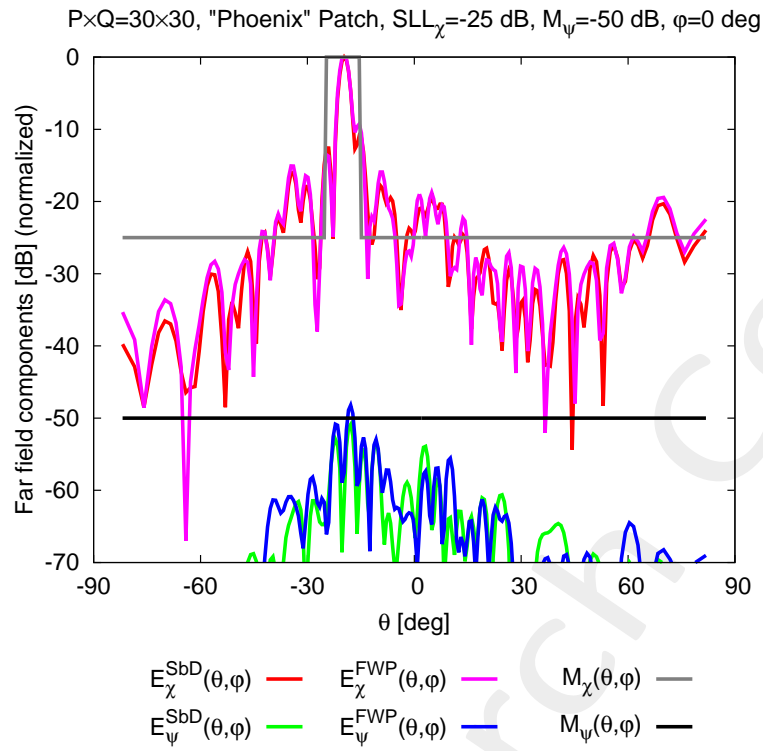


Figure 7: Phoenix Patch Reflectarray 30×30 SLL=-25 dB - Optimization - Radiated Field Cut with the comparison.

2 Phoenix Patch Reflectarray: 35x35 SLL=-25dB

2.1 Optimization target

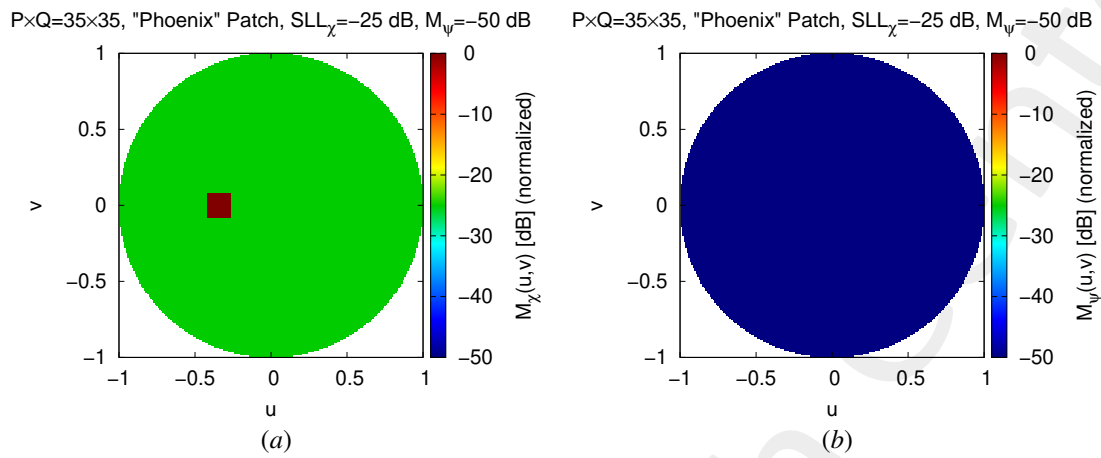


Figure 8: Phoenix Patch Reflectarray 35×35 SLL=-25 dB - Optimization target: SLL on the wanted polarization(a), mask on the unwanted polarization (b).

2.2 Optimization results

2.2.1 Cost Function

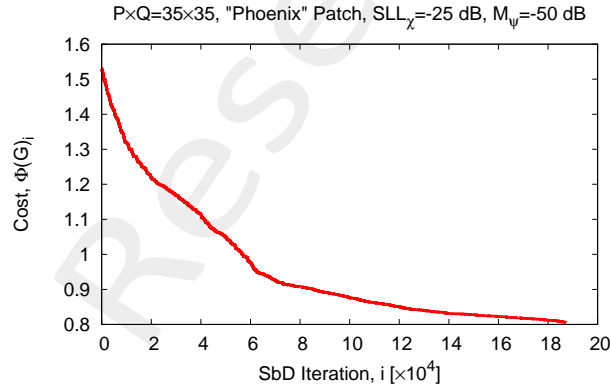


Figure 9: Phoenix Patch Reflectarray 35×35 SLL=-25 dB - Optimization: Cost function behavior.

2.2.2 Geometrical Design

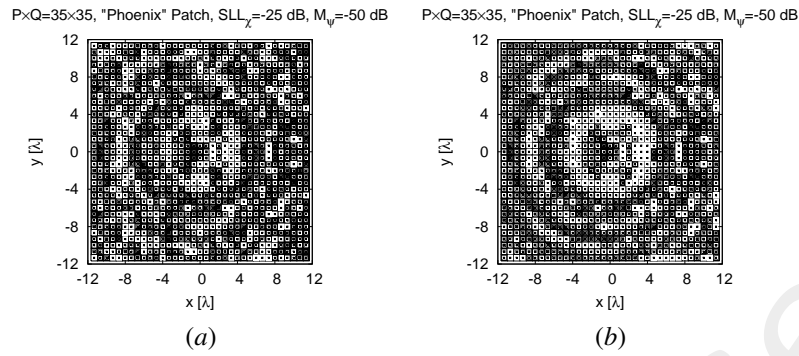


Figure 10: Phoenix Patch Reflectarray 35×35 SLL=-25 dB - Optimization: Starting reflectarray configuration(a) and optimized reflectarray configuration (b).

2.2.3 Reflection Coefficient

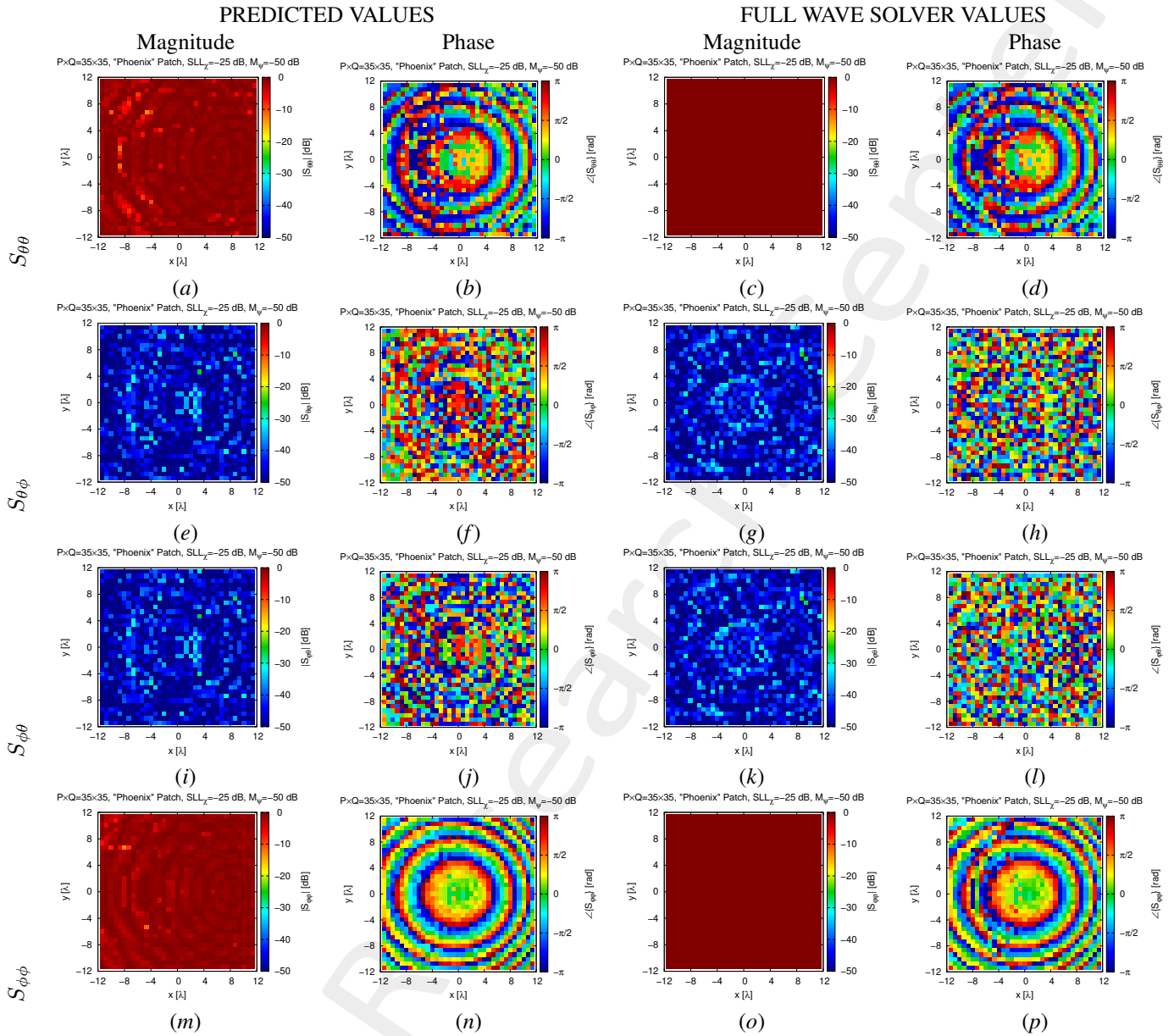


Figure 11: Phoenix Patch Reflectarray 35×35 SLL=-25 dB - Optimization - Reflection Coefficients: predicted(a)(b)(e)(f)(i)(j)(m)(n) vs. full-wave simulation (c)(d)(g)(h)(k)(l)(o)(p) of the magnitude(a)(c)(e)(g)(i)(k)(m)(o) and phase (b)(d)(f)(h)(j)(l)(n)(p) of $S_{\theta\theta}$ (a)(b)(c)(d), $S_{\theta\phi}$ (e)(f)(g)(h), $S_{\phi\theta}$ (i)(j)(k)(l) and $S_{\phi\phi}$ (m)(n)(o)(p).

2.2.4 Superficial Currents

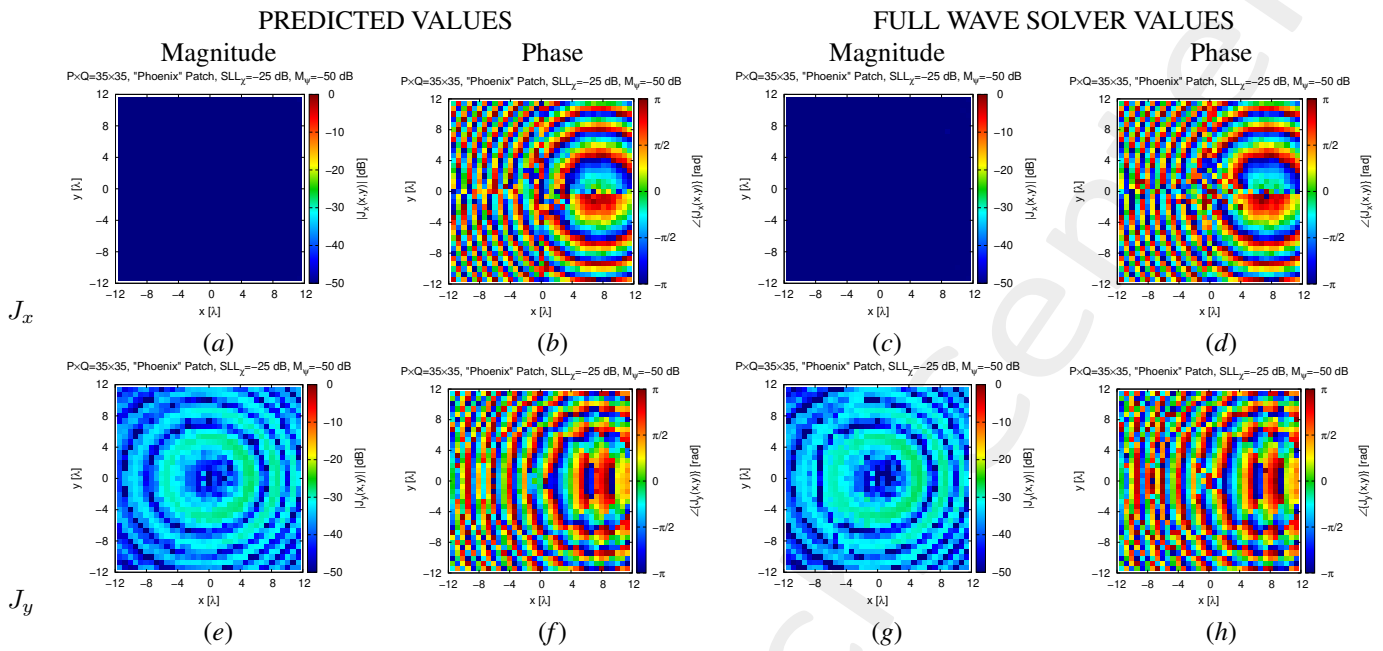


Figure 12: Phoenix Patch Reflectarray 35×35 SLL=-25 dB - Optimization - Superficial Currents: predicted(a)(b)(e)(f) vs. full-wave simulation (c)(d)(g)(h) of the magnitude(a)(c)(e)(g) and phase (b)(d)(f)(h) of J_x (a)(b)(c)(d) and J_y (e)(f)(g)(h).

2.2.5 Fields

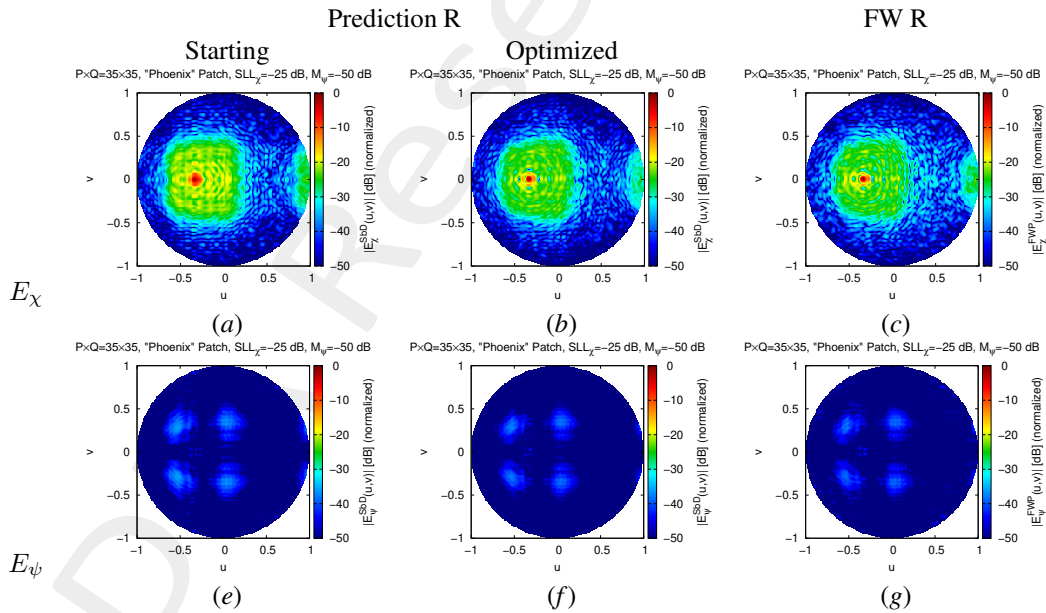


Figure 13: Phoenix Patch Reflectarray 35×35 SLL=-25 dB - Optimization - Radiated Fields: predicted(a)(b)(e)(f) vs. full-wave simulation of R (c)(g) vs. full-wave simulation of the entire structure (d)(h) of the magnitude of E_χ (a)(b)(c)(d) and E_ψ (e)(f)(g)(h).

2.2.6 Fields Cut

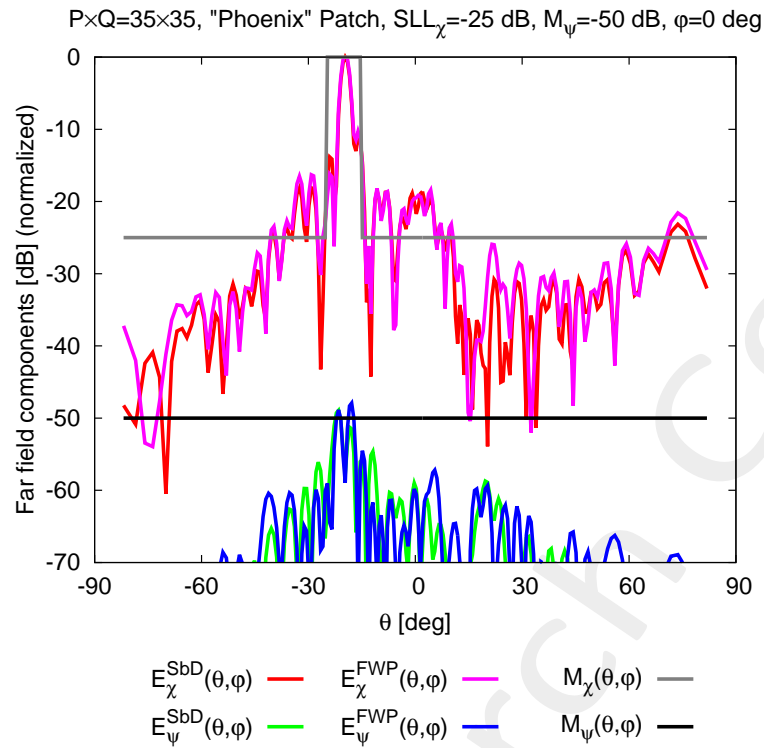


Figure 14: Phoenix Patch Reflectarray 35×35 SLL=-25 dB - Optimization - Radiated Field Cut with the comparison.

3 Double Layer Square Patch Reflectarray: 29x29

3.1 Unit cell geometry

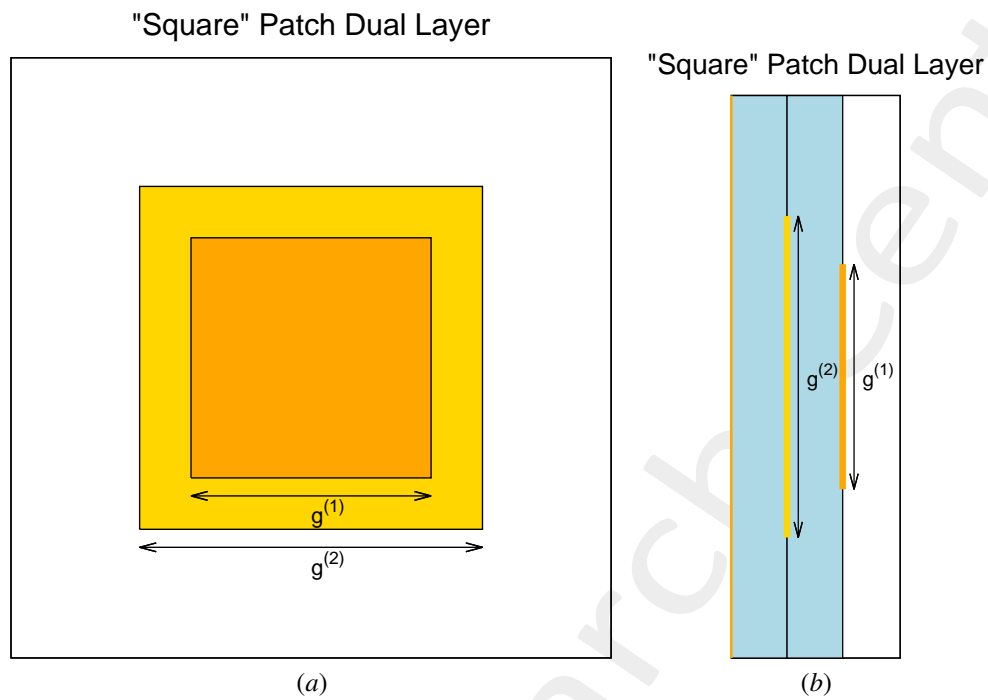


Figure 15: Square Patch Dual Layer unit cell, front (a) and side (b) view.

3.2 Optimization target

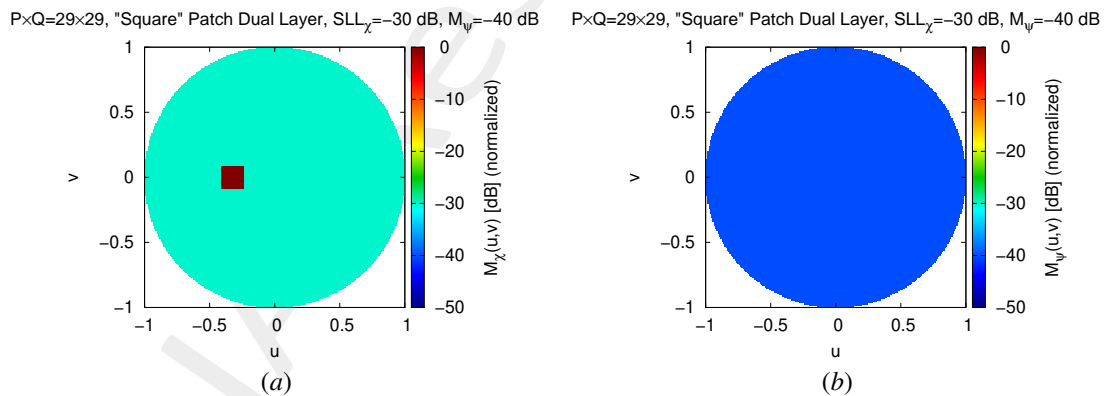


Figure 16: Double Layer Square Patch Reflectarray 29×29 $\alpha_{\beta} = \alpha_{\Gamma} = 1.0$ - Optimization target: SLL on the wanted polarization(a), mask on the unwanted polarization (b).

3.3 Optimization results

3.3.1 Cost Function

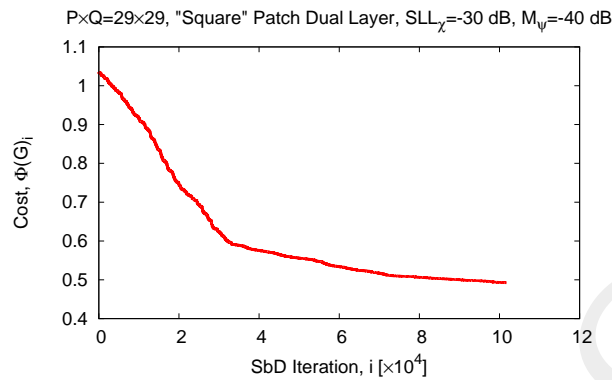


Figure 17: Double Layer Square Patch Reflectarray 29×29 $\alpha_{\beta} = \alpha_{\Gamma} = 1.0$ - Optimization: Cost function behavior.

3.3.2 Geometrical Design

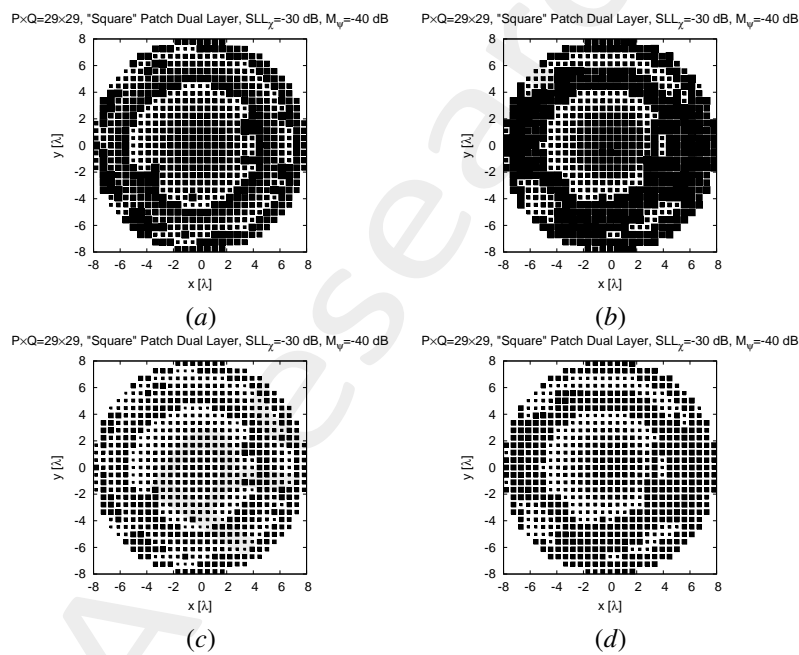


Figure 18: Double Layer Square Patch Reflectarray 29×29 $\alpha_{\beta} = \alpha_{\Gamma} = 1.0$ - Optimization: Starting reflectarray configuration(a)(c), optimized reflectarray configuration (b)(d) for layer one (a)(b) and layer two (c)(d).

3.3.3 Reflection Coefficient

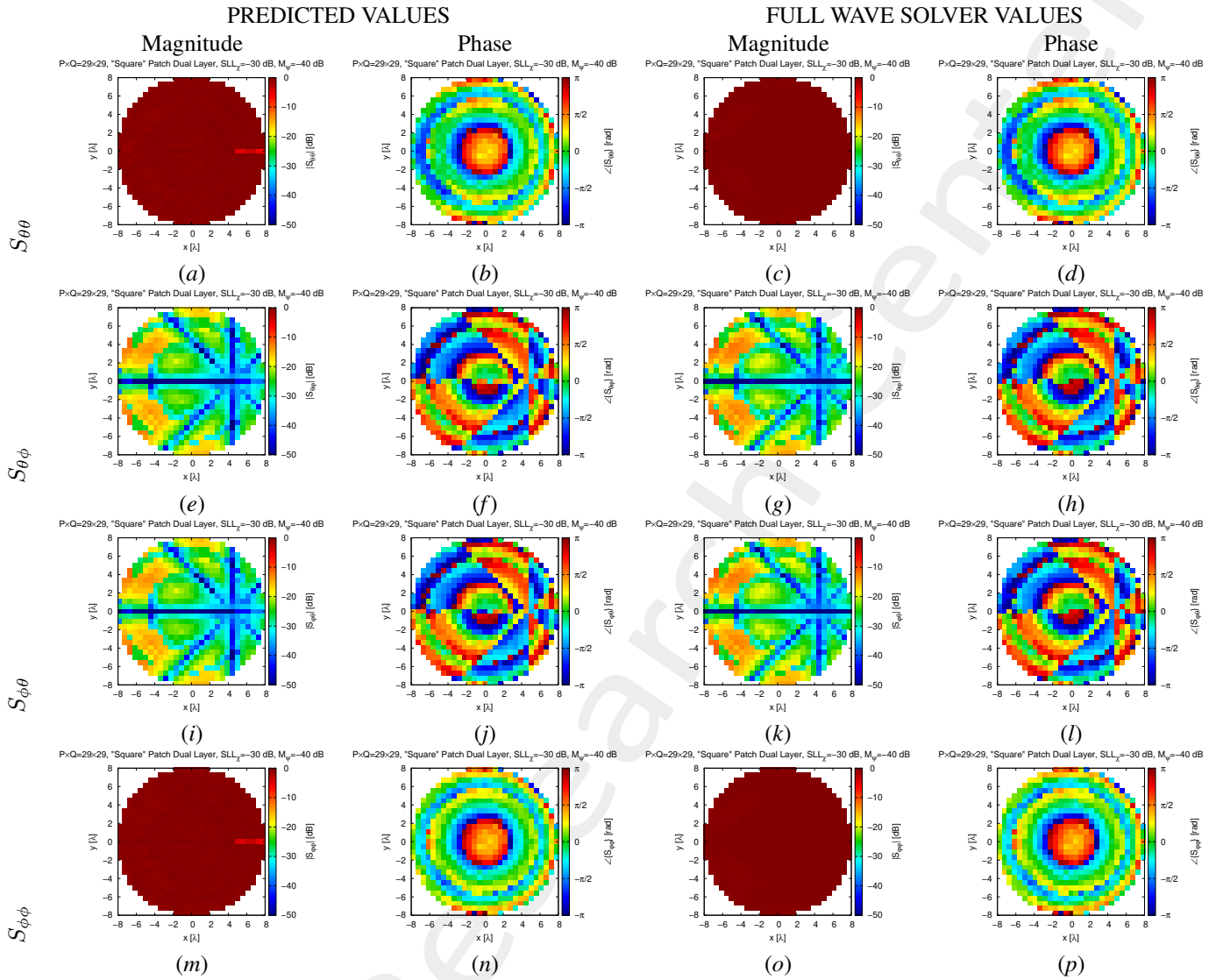


Figure 19: Double Layer Square Patch Reflectarray 29×29 $\alpha_\beta = \alpha_\Gamma = 1.0$ - Optimization - Reflection Coefficients: predicted(a)(b)(e)(f)(i)(j)(m)(n) vs. full-wave simulation (c)(d)(g)(h)(k)(l)(o)(p) of the magnitude(a)(c)(e)(g)(i)(k)(m)(o) and phase (b)(d)(f)(h)(j)(l)(n)(p) of $S_{\theta\theta}$ (a)(b)(c)(d), $S_{\theta\phi}$ (e)(f)(g)(h), $S_{\phi\theta}$ (i)(j)(k)(l) and $S_{\phi\phi}$ (m)(n)(o)(p).

3.3.4 Superficial Currents

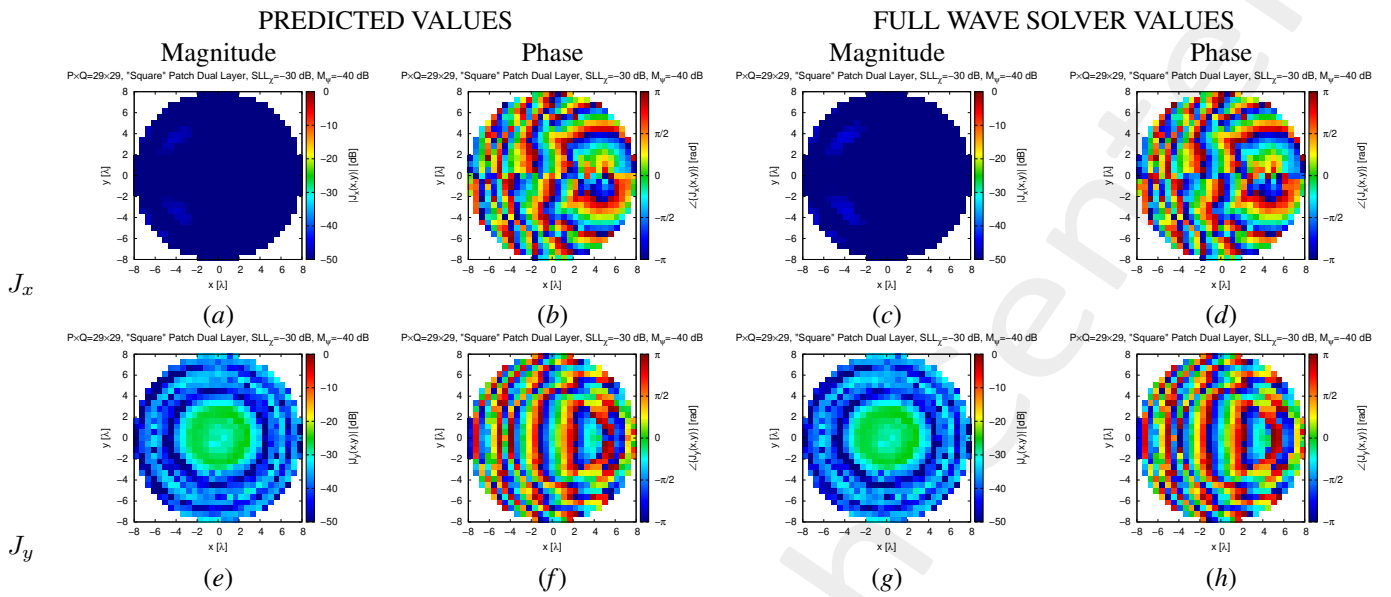


Figure 20: Double Layer Square Patch Reflectarray 29×29 $\alpha_\beta = \alpha_\Gamma = 1.0$ - Optimization - Superficial Currents: predicted(a)(b)(e)(f) vs. full-wave simulation (c)(d)(g)(h) of the magnitude(a)(c)(e)(g) and phase (b)(d)(f)(h) of J_x (a)(b)(c)(d) and J_y (e)(f)(g)(h).

3.3.5 Fields

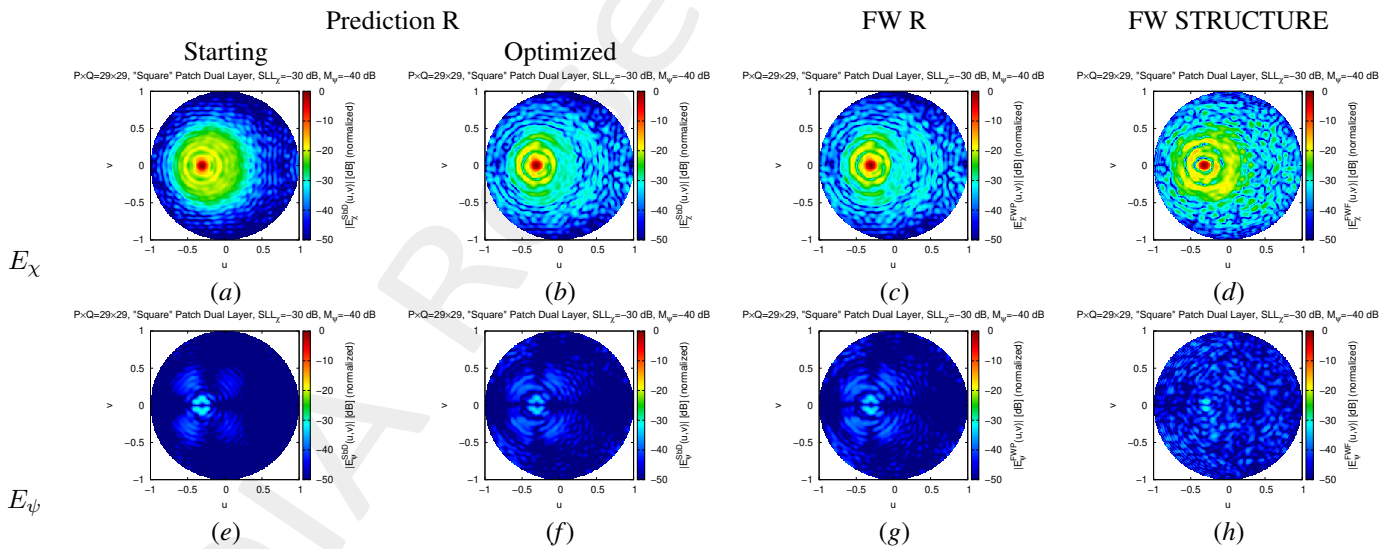


Figure 21: Double Layer Square Patch Reflectarray 29×29 $\alpha_\beta = \alpha_\Gamma = 1.0$ - Optimization - Radiated Fields: predicted(a)(b)(e)(f) vs. full-wave simulation of R (c)(g) vs. full-wave simulation of the entire structure (d)(h) of the magnitude of E_x (a)(b)(c)(d) and E_ψ (e)(f)(g)(h).

3.3.6 Fields Cut

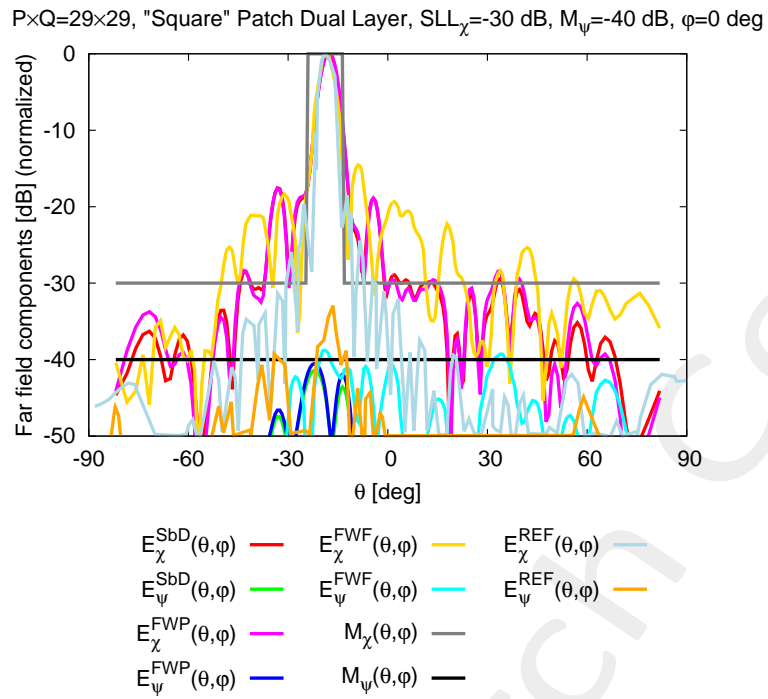


Figure 22: Double Layer Square Patch Reflectarray 29×29 $\alpha_{\beta} = \alpha_{\Gamma} = 1.0$ - Optimization - Radiated Field Cut with the comparison.

4 Double Layer Square Patch Reflectarray: 29x29, Similarity Weight=10

4.1 Optimization target

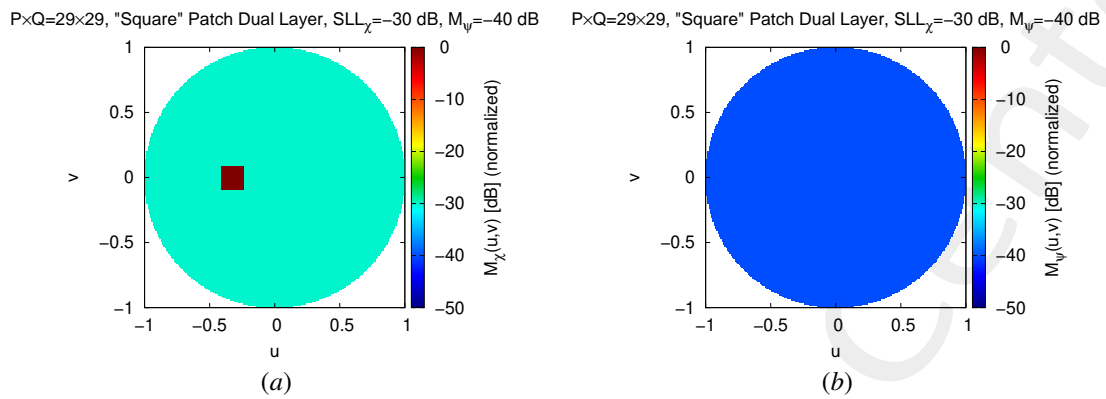


Figure 23: Double Layer Square Patch Reflectarray 29×29 $\alpha_\beta = 1.0$, $\alpha_\Gamma = 10.0$ - Optimization target: SLL on the wanted polarization(a), mask on the unwanted polarization (b).

4.2 Optimization results

4.2.1 Cost Function

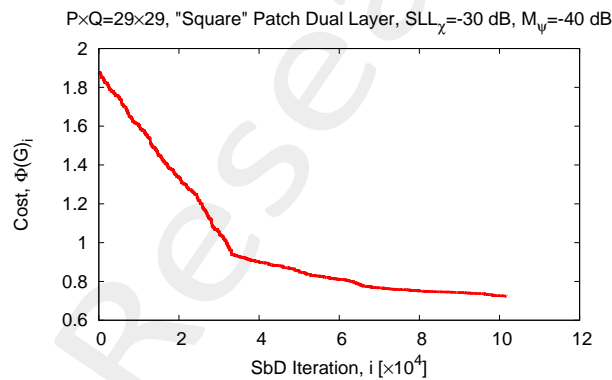


Figure 24: Double Layer Square Patch Reflectarray 29×29 $\alpha_\beta = 1.0$, $\alpha_\Gamma = 10.0$ - Optimization: Cost function behavior.

4.2.2 Geometrical Design

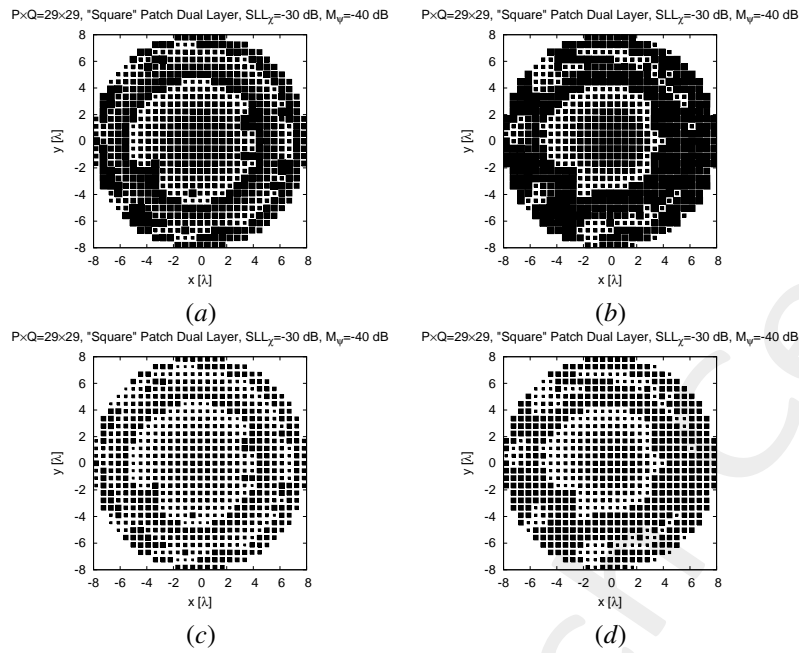


Figure 25: Double Layer Square Patch Reflectarray 29×29 $\alpha_\beta = 1.0$, $\alpha_\Gamma = 10.0$ - Optimization: Starting reflectarray configuration (a)(c), optimized reflectarray configuration (b)(d) for layer one (a)(b) and layer two (c)(d).

4.2.3 Reflection Coefficient

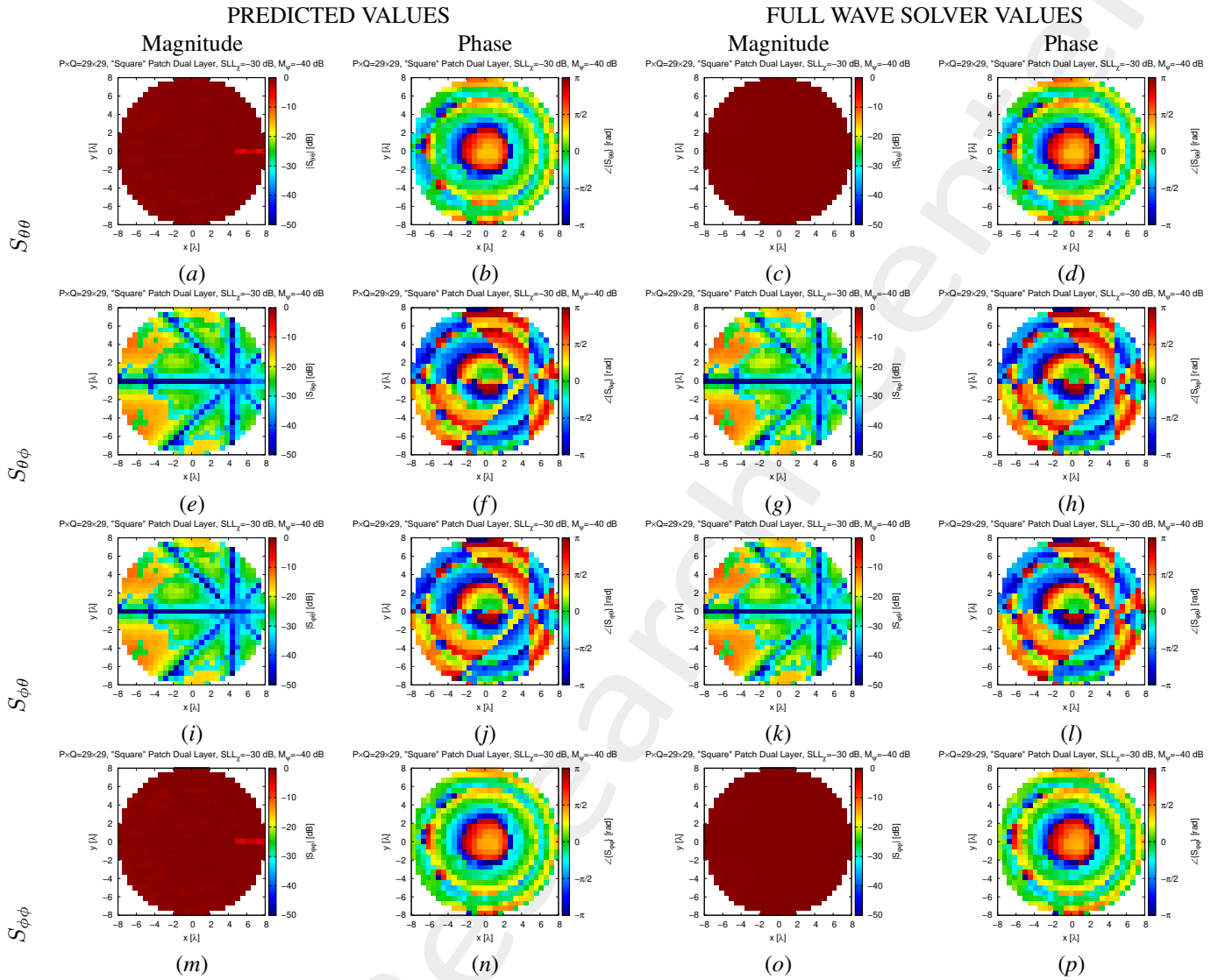


Figure 26: Double Layer Square Patch Reflectarray 29×29 $\alpha_\beta = 1.0$, $\alpha_\Gamma = 10.0$ - Optimization - Reflection Coefficients: predicted(a)(b)(e)(f)(i)(j)(m)(n) vs. full-wave simulation (c)(d)(g)(h)(k)(l)(o)(p) of the magnitude(a)(c)(e)(g)(i)(k)(m)(o) and phase (b)(d)(f)(h)(j)(l)(n)(p) of $S_{\theta\theta}$ (a)(b)(c)(d), $S_{\theta\phi}$ (e)(f)(g)(h), $S_{\phi\theta}$ (i)(j)(k)(l) and $S_{\phi\phi}$ (m)(n)(o)(p).

4.2.4 Superficial Currents

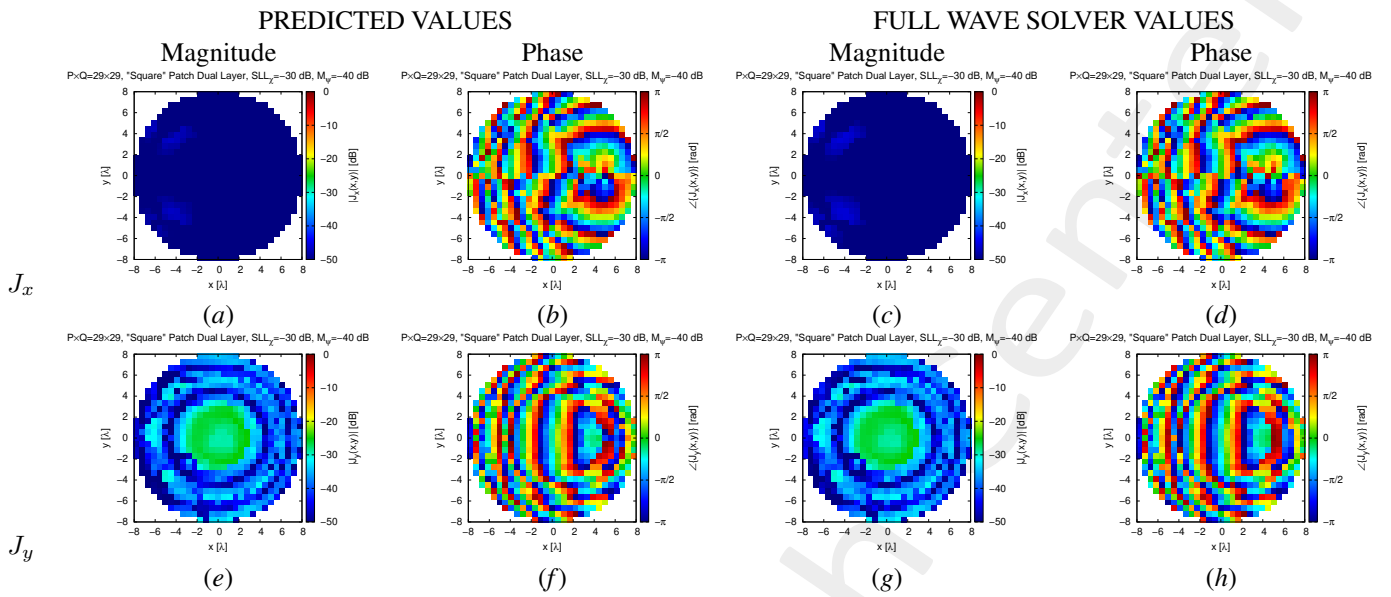


Figure 27: Double Layer Square Patch Reflectarray 29×29 $\alpha_\beta = 1.0$, $\alpha_\Gamma = 10.0$ - Optimization - Superficial Currents: predicted(a)(b)(e)(f) vs. full-wave simulation (c)(d)(g)(h)of the magnitude(a)(c)(e)(g) and phase (b)(d)(f)(h) of J_x (a)(b)(c)(d) and J_y (e)(f)(g)(h).

4.2.5 Fields

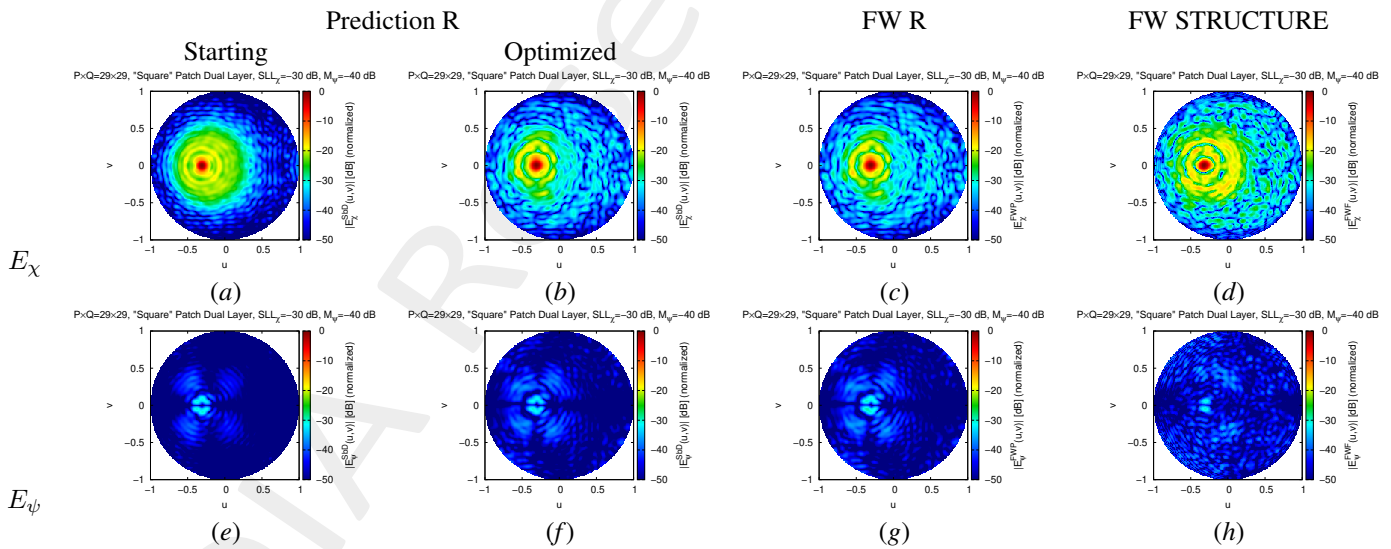


Figure 28: Double Layer Square Patch Reflectarray 29×29 $\alpha_\beta = 1.0$, $\alpha_\Gamma = 10.0$ - Optimization - Radiated Fields: predicted(a)(b)(e)(f) vs. full-wave simulation of R (c)(g) vs. full-wave simulation of the entire structure (d)(h) of the magnitude of E_x (a)(b)(c)(d) and E_ψ (e)(f)(g)(h).

4.2.6 Fields Cut

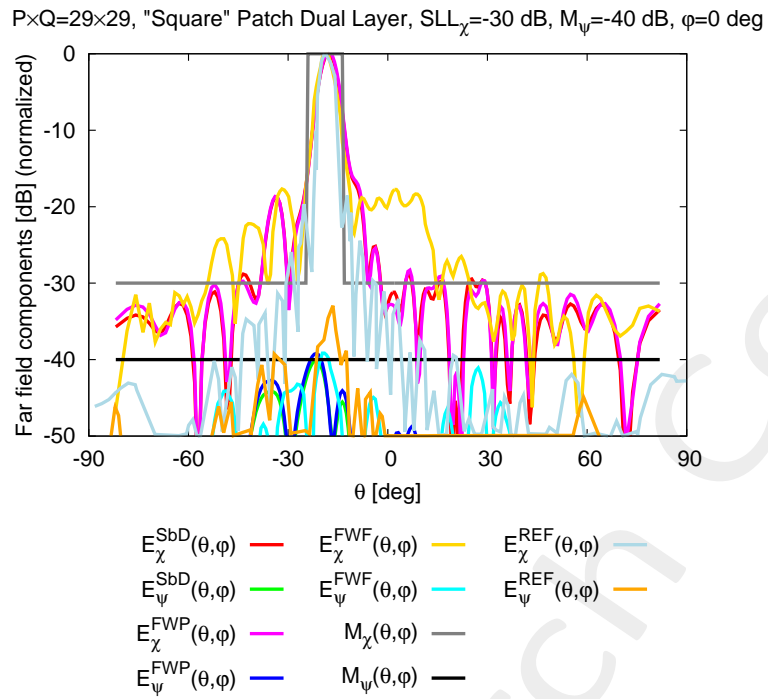


Figure 29: Double Layer Square Patch Reflectarray 29×29 $\alpha_{\beta} = 1.0$, $\alpha_{\Gamma} = 10.0$ - Optimization - Radiated Field Cut with the comparison .

More information on the topics of this document can be found in the following list of references.

References

- [1] P. Rocca, M. Benedetti, M. Donelli, D. Franceschini, and A. Massa, "Evolutionary optimization as applied to inverse problems," *Inverse Problems - 25 th Year Special Issue of Inverse Problems, Invited Topical Review*, vol. 25, pp. 1-41, Dec. 2009.
- [2] P. Rocca, G. Oliveri, and A. Massa, "Differential Evolution as applied to electromagnetics," *IEEE Antennas Propag. Mag.*, vol. 53, no. 1, pp. 38-49, Feb. 2011.
- [3] P. Rocca, N. Anselmi, A. Polo, and A. Massa, "An irregular two-sizes square tiling method for the design of isophoric phased arrays," *IEEE Trans. Antennas Propag.*, vol. 68, no. 6, pp. 4437-4449, Jun. 2020.
- [4] P. Rocca, N. Anselmi, A. Polo, and A. Massa, "Modular design of hexagonal phased arrays through diamond tiles," *IEEE Trans. Antennas Propag.*, vol.68, no. 5, pp. 3598-3612, May 2020.
- [5] N. Anselmi, L. Poli, P. Rocca, and A. Massa, "Design of simplified array layouts for preliminary experimental testing and validation of large AESAs," *IEEE Trans. Antennas Propag.*, vol. 66, no. 12, pp. 6906-6920, Dec. 2018.
- [6] N. Anselmi, P. Rocca, M. Salucci, and A. Massa, "Contiguous phase-clustering in multibeam-on-receive scanning arrays," *IEEE Trans. Antennas Propag.*, vol. 66, no. 11, pp. 5879-5891, Nov. 2018.
- [7] G. Oliveri, G. Gottardi, F. Robol, A. Polo, L. Poli, M. Salucci, M. Chuan, C. Massagrande, P. Vinetti, M. Mattivi, R. Lombardi, and A. Massa, "Co-design of unconventional array architectures and antenna elements for 5G base station," *IEEE Trans. Antennas Propag.*, vol. 65, no. 12, pp. 6752-6767, Dec. 2017.
- [8] N. Anselmi, P. Rocca, M. Salucci, and A. Massa, "Irregular phased array tiling by means of analytic schemata-driven optimization," *IEEE Trans. Antennas Propag.*, vol. 65, no. 9, pp. 4495-4510, September 2017.
- [9] N. Anselmi, P. Rocca, M. Salucci, and A. Massa, "Optimization of excitation tolerances for robust beamforming in linear arrays," *IET Microwaves, Antennas & Propagation*, vol. 10, no. 2, pp. 208-214, 2016.
- [10] P. Rocca, R. J. Mailloux, and G. Toso, "GA-Based optimization of irregular sub-array layouts for wideband phased arrays design," *IEEE Antennas and Wireless Propag. Lett.*, vol. 14, pp. 131-134, 2015.
- [11] P. Rocca, M. Donelli, G. Oliveri, F. Viani, and A. Massa, "Reconfigurable sum-difference pattern by means of parasitic elements for forward-looking monopulse radar," *IET Radar, Sonar & Navigation*, vol 7, no. 7, pp. 747-754, 2013.
- [12] P. Rocca, L. Manica, and A. Massa, "Ant colony based hybrid approach for optimal compromise sum-difference patterns synthesis," *Microwave Opt. Technol. Lett.*, vol. 52, no. 1, pp. 128-132, Jan. 2010.
- [13] P. Rocca, L. Manica, and A. Massa, "An improved excitation matching method based on an ant colony optimization for suboptimal-free clustering in sum-difference compromise synthesis," *IEEE Trans. Antennas Propag.*, vol. 57, no. 8, pp. 2297-2306, Aug. 2009.

-
- [14] P. Rocca, L. Manica, and A. Massa, "Hybrid approach for sub-arrayed monopulse antenna synthesis," *Electronics Letters*, vol. 44, no. 2, pp. 75-76, Jan. 2008.
- [15] P. Rocca, L. Manica, F. Stringari, and A. Massa, "Ant colony optimization for tree-searching based synthesis of monopulse array antenna," *Electronics Letters*, vol. 44, no. 13, pp. 783-785, Jun. 19, 2008.
- [16] G. Oliveri, A. Gelmini, A. Polo, N. Anselmi, and A. Massa, "System-by-design multi-scale synthesis of task-oriented reflectarrays," *IEEE Trans. Antennas Propag.*, vol. 68, no. 4, pp. 2867-2882, Apr. 2020.
- [17] M. Salucci, F. Robol, N. Anselmi, M. A. Hannan, P. Rocca, G. Oliveri, M. Donelli, and A. Massa, "S-Band spline-shaped aperture-stacked patch antenna for air traffic control applications," *IEEE Tran. Antennas Propag.*, vol. 66, no. 8, pp. 4292-4297, Aug. 2018.
- [18] M. Salucci, L. Poli, A. F. Morabito, and P. Rocca, "Adaptive nulling through subarray switching in planar antenna arrays," *Journal of Electromagnetic Waves and Applications*, vol. 30, no. 3, pp. 404-414, February 2016
- [19] T. Moriyama, L. Poli, and P. Rocca, "Adaptive nulling in thinned planar arrays through genetic algorithms," *IEICE Electronics Express*, vol. 11, no. 21, pp. 1-9, Sep. 2014.
- [20] L. Poli, P. Rocca, M. Salucci, and A. Massa, "Reconfigurable thinning for the adaptive control of linear arrays," *IEEE Trans. Antennas Propag.*, vol. 61, no. 10, pp. 5068-5077, Oct. 2013.
- [21] P. Rocca, L. Poli, G. Oliveri, and A. Massa, "Adaptive nulling in time-varying scenarios through time-modulated linear arrays," *IEEE Antennas Wireless Propag. Lett.*, vol. 11, pp. 101-104, 2012.
- [22] M. Benedetti, G. Oliveri, P. Rocca, and A. Massa, "A fully-adaptive smart antenna prototype: ideal model and experimental validation in complex interference scenarios," *Progress in Electromagnetic Research*, PIER 96, pp. 173-191, 2009.
- [23] M. Benedetti, R. Azaro, and A. Massa, "Memory enhanced PSO-based optimization approach for smart antennas control in complex interference scenarios," *IEEE Trans. Antennas Propag.*, vol. 56, no. 7, pp. 1939-1947, Jul. 2008.
- [24] M. Benedetti, R. Azaro, and A. Massa, "Experimental validation of a fully-adaptive smart antenna prototype," *Electronics Letters*, vol. 44, no. 11, pp. 661-662, May 2008.
- [25] R. Azaro, L. Ioriatti, M. Martinelli, M. Benedetti, and A. Massa, "An experimental realization of a fully-adaptive smart antenna," *Microwave Opt. Technol. Lett.*, vol. 50, no. 6, pp. 1715-1716, Jun. 2008.
- [26] M. Donelli, R. Azaro, L. Fimognari, and A. Massa, "A planar electronically reconfigurable Wi-Fi band antenna based on a parasitic microstrip structure," *IEEE Antennas Wireless Propag. Lett.*, vol. 6, pp. 623-626, 2007.
- [27] M. Benedetti, R. Azaro, D. Franceschini, and A. Massa, "PSO-based real-time control of planar uniform circular arrays," *IEEE Antennas Wireless Propag. Lett.*, vol. 5, pp. 545-548, 2006.
- [28] G. Oliveri, P. Rocca, M. Salucci, and A. Massa, "Holographic smart EM skins for advanced beam power shaping in next generation wireless environments," *IEEE J. Multiscale Multiphysics Comput. Tech.*, vol. 6, pp. 171-182, Oct. 2021.

-
- [29] M. Salucci, L. Tenuti, G. Gottardi, A. Hannan, and A. Massa, "System-by-design method for efficient linear array miniaturisation through low-complexity isotropic lenses," *Electronic Letters*, vol. 55, no. 8, pp. 433-434, May 2019.
- [30] M. Salucci, N. Anselmi, S. Goudos, and A. Massa, "Fast design of multiband fractal antennas through a system-by-design approach for NB-IoT applications," *EURASIP J. Wirel. Commun. Netw.*, vol. 2019, no. 1, pp. 68-83, Mar. 2019.
- [31] M. Salucci, G. Oliveri, N. Anselmi, and A. Massa, "Material-by-design synthesis of conformal miniaturized linear phased arrays," *IEEE Access*, vol. 6, pp. 26367-26382, 2018.
- [32] M. Salucci, G. Oliveri, N. Anselmi, G. Gottardi, and A. Massa, "Performance enhancement of linear active electronically-scanned arrays by means of MbD-synthesized metalenses," *Journal of Electromagnetic Waves and Applications*, vol. 32, no. 8, pp. 927-955, 2018.
- [33] G. Oliveri, M. Salucci, N. Anselmi and A. Massa, "Multiscale System-by-Design synthesis of printed WAIMs for waveguide array enhancement," *IEEE J. Multiscale Multiphysics Computat. Techn.*, vol. 2, pp. 84-96, 2017.
- [34] A. Massa and G. Oliveri, "Metamaterial-by-Design: Theory, methods, and applications to communications and sensing - Editorial," *EPJ Applied Metamaterials*, vol. 3, no. E1, pp. 1-3, 2016.
- [35] G. Oliveri, F. Viani, N. Anselmi, and A. Massa, "Synthesis of multi-layer WAIM coatings for planar phased arrays within the system-by-design framework," *IEEE Trans. Antennas Propag.*, vol. 63, no. 6, pp. 2482-2496, June 2015.
- [36] G. Oliveri, L. Tenuti, E. Bekele, M. Carlin, and A. Massa, "An SbD-QCTO approach to the synthesis of isotropic metamaterial lenses," *IEEE Antennas Wireless Propag. Lett.*, vol. 13, pp. 1783-1786, 2014.
- [37] A. Massa, G. Oliveri, P. Rocca, and F. Viani, "System-by-Design: a new paradigm for handling design complexity," *8th European Conference on Antennas Propag. (EuCAP 2014)*, The Hague, The Netherlands, pp. 1180-1183, Apr. 6-11, 2014.
- [38] P. Rocca, G. Oliveri, R. J. Mailloux, and A. Massa, "Unconventional phased array architectures and design Methodologies - A review," *Proceedings of the IEEE*, vol. 104, no. 3, pp. 544-560, March 2016.